ESTIMATION OF PARTIAL SOUND SOURCES WITH NON-SPHERICAL DIRECTIVITY FOR ANALYSIS OF PASS-BY NOISE IN HEMI-ANECHOIC INDOOR TEST BENCHES

Christof Puhle[1], Volker Becker[1], Alexander Jahnke[1] and Fabian Knappe[2]

[1]GFaI e. V.
Volmerstraße 3, 12489, Berlin, Germany
[2]NEXT Data Service AG
Alt-Moabit 104, 10559 Berlin, Germany

ABSTRACT

Partial sound source estimation of complex acoustic scenarios is a common problem in automotive acoustics. Transfer Path Analysis based approaches, e.g., Airborne Source Quantification (ASQ), still show various limitations. ASQ is used to quantify the partial sound sources of motor vehicles' exterior noise, also known as pass-by noise, at hemi-anechoic indoor test benches. The legal requirements on the regulations of pass-by noise, including the latest Economic Commission for Europe (ECE) R51.03 test, are continuously rising. Thus, there is a need for more precise analysis of the influence of different vehicle components on the exterior noise. One of the limitations of ASQ, the monopole assumption, is addressed by the authors' algorithm for partial sound source estimation of pass-by noise, called Helmholtz Inverse Beamforming (HIBF). Instead of omnidirectional sources, HIBF uses spherical harmonics representation of the partial sound sources. The development of HIBF is embedded in a comprehensive research project, targeting the complete digitalization of pass-by noise engineering. This paper presents a comparison of HIBF with ASQ. In particular, the results are validated for synthetic measurements and operational vehicle measurements.

1 INTRODUCTION

The necessity of governmental regulations on exterior noise emissions of motor vehicles, also known as pass-by, comes from the general impact of noise on human health. Pass-by noise has gained a high interest in automotive engineering in the prior decade. This is a result of continuously rising requirements on the regulations of noise emissions. The latest Economic Commission for Europe (ECE)-Homologation process is based on the ECE R51.03 test [1]. Compared to the previous version, the ECE R51.02, one of the major new features is a

completely updated test procedure. The development of the ECE R51.03 is based on in-use driving statistics to address the insufficient representation of the in-use behavior of the ECE R51.02 [2]. As mentioned above the updated test procedure consists of more restrictive thresholds that future cars must adhere to. Thus, one of the key features of future acoustic engineering is gaining higher flexibility concerning adaptions of the vehicles' acoustic behavior to fulfill the governmental pass-by regulations. To be efficient in manipulating the over-all exterior noise of motor vehicles, more detailed information of their partial sound sources is needed. Additionally, digitalization has changed the world of original equipment manufacturers (OEMs) in various aspects. There is a shift in automotive engineering from physical hardware to digital representations of the expected physical behavior of future cars. The previous enablers for more efficient manufacturing, e.g., optimized production lines have experienced enlargement related to information and communication services (ICT) [3].

1.1   Background

The presented study is part of a comprehensive research project. The overlying project includes cooperation from Mercedes-Benz AG with Society for the Advancement of Applied Computer Science (GFaI e.V.), DataZoo GmbH and Next Data Service AG. The main goal of the project is the derivation of individual acoustic thresholds of different car components in the early, digital stages of the product development process [4, 5]. Therefore, digital twins in form of machine learning (ML) models and acoustic techniques are combined. The project consists of two main algorithms. The first one, called Helmholtz Inverse Beamforming (HIBF), is presented in this study. HIBF is a new technique for partial sound source estimation. The second key component of the pass-by noise digitalization project consists of ML approaches. The pass-by noise of future cars is predicted via gradient boosted models (GBMs) [6].

1.2   Problem formulation

Optimizing the vibro-acoustics performance of motor vehicles, also known as Noise, Vibration, Harshness (NVH) is a challenging task in automotive engineering. Most acoustic phenomena appearing in the context of automobiles consist of numerous simultaneous excitations and complex transmission paths. Transfer Path Analysis (TPA) is the most common approach to identify the main acoustic sources and their transfer paths of machines with complex acoustic behavior. According to [7] TPA techniques can be separated in two main classes and corresponding subclasses. The first class of algorithms estimates the partial sound pressure contributions of airborne sources (Airborne TPA), while the second class regards structural forces as well (Structural TPA). According to [7] the most widely used techniques within Airborne TPA are "windowing" techniques, substitution monopole techniques, matrix inversion methods, direct particle velocity measurements, beamforming and holographic technologies using pressure arrays. Also, in the case of pass-by noise analysis TPA is a widely used technique among NVH engineers [8] [9] [10]. Though there are existing technologies addressing the separation of acoustic sources with overlapping frequency range, e.g., beamforming, where sources are separated with microphone arrays and spatial filters [11], these technologies do not provide real acoustic source descriptions, e.g., by their acoustic volume velocities. Beamforming rather gives a relative intuition of the different effect strengths of the sources in form of the sound pressure level (SPL) at the microphone array. Thus, these technologies cannot be used for virtual manipulation of different sources, e.g., by changing their

directivities or volume velocities. For that reason, the authors developed HIBF, a new algorithm for partial sound source estimation of sources with non-spherical directivities.

2   ECE-HOMOLOGATION

The legal requirements for measuring pass-by noise are strictly regulated. Figure 1 shows the measurement configuration for pass-by of motor vehicles according to ISO 362 [12].
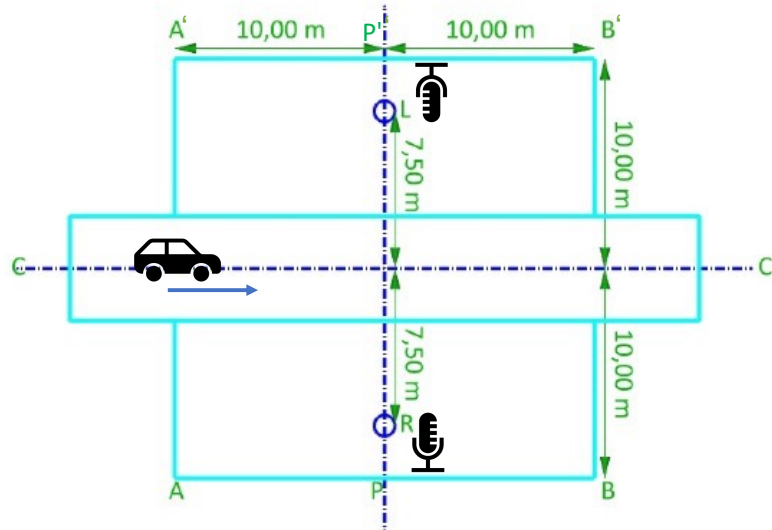

Fig. 1 Pass-by measurement area according to ISO 362. Start / stop of measurements is triggered by the car passing line AA' / line BB'. The trajectory of the car is defined by line CC'. Along line PP' with 7.5 m distance from line CC' two microphones are placed in a height of 1.2 m.

The ECE R51.03 [1], the latest series of amendments, was developed because the ECE 51.02 was no longer suitable for measuring pass-by noise under representative conditions. Measurements according to ECE 51.02 are performed under full longitudinal acceleration of cars (not representing typical urban driving situations) [2]. For that reason, homologations according to ECE R51.03 are performed differently. Depending on multiple car parameters, such as vehicle mass, engine power and the acceleration of the car, the legal regulations demand measurements in more than one gear [1]. For reasons of simplicity at this point the procedure will only be described for examples where measurements in a single gear i are sufficient.
The following tests must be performed:

- Constant pass-by: The car must have a speed of 13.9 ± 0.3 m/s between the lines AA' and BB'.

- Accelerated pass-by: When the reference point of the car passes the AA' line the driver fully accelerates until passing the BB' line. The speed of the car must be 13.9 ± 0.3 m/s at line PP'.

The relevant value of each measurement is the A-weighted SPL. Four consecutive measurements, so-called runs, with a maximum divergence of 2 dB must be recorded. The results are averaged for both microphones and the louder average is chosen. With the resulting values $L_{crs\,i}$ (for constant runs) and $L_{wot\,i}$ (for accelerated runs) two representative values ($L_{wot\,rep}$ and $L_{crs\,rep}$) are derived. Finally, L_{urban}, which represents the SPL at the typical

urban acceleration (a_{urban}) is calculated [1]. L_{urban} can be interpreted as an interpolation on a line from $L_{crs\ rep}$ to $L_{wot\ rep}$.

3   AIRBORNE SOURCE QUANTIFICATION

Pass-by noise measurements are typically performed on outdoor test tracks. Nevertheless pass-by noise can also be measured indoors at hemi-anechoic test chambers. In this case two lines of microphones are used to reverse the relation of the movement, i.e., instead of a moving car a virtual microphone is moved via crossfading of the real microphones. This process is called simulated pass-by. This gives NVH engineers the opportunity to perform measurements under very reproducible and stable conditions. Furthermore, indoor measurements offer the possibility of applying additional measurement hardware, e.g., microphones, around the vehicle to perform more detailed analysis of the acoustic behavior. The idea of ASQ in form of source-path-receiver models is known for many decades [13]. Figure 2 shows the principle of ASQ.
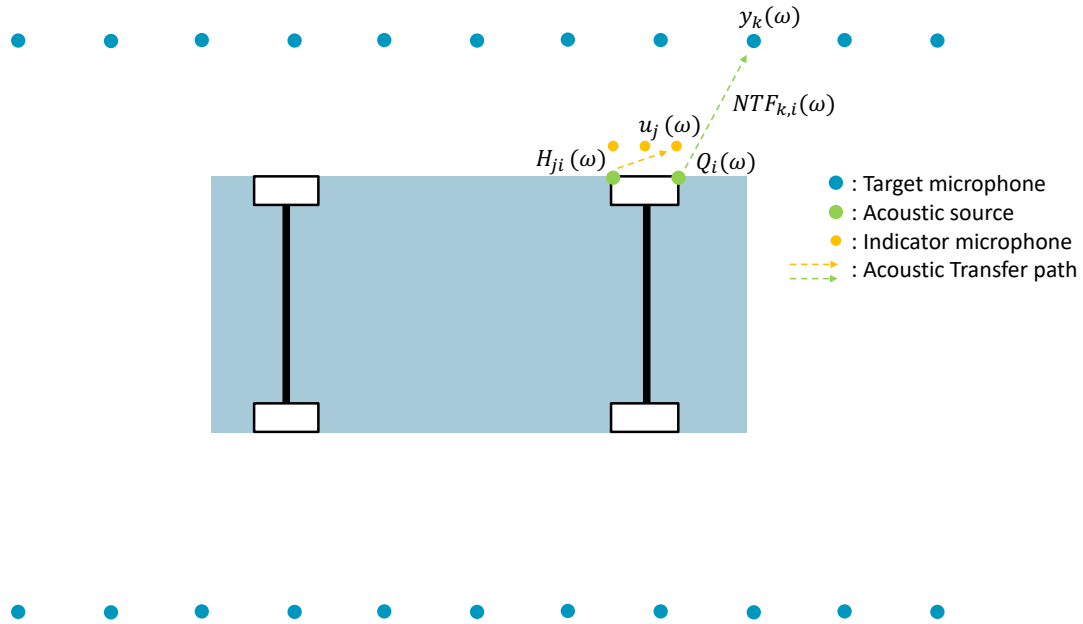

Fig. 2. Principle of ASQ for pass-by noise according to [8]. The vehicle is measured indoors in a hemi-anechoic chamber. Acoustic loads are estimated via indicator microphones. The sound pressure levels at the target microphones for simulated pass-by are estimated via the acoustic loads.

According to [8] the power-based ASQ approach can be mathematically formulated via Eq. (1):

$$y_k^2(\omega) = \sum_{i=1}^{n} NTF_{ki}^2(\omega) \cdot Q_i^2(\omega) \tag{1}$$

where y_k is the sum of the sound signal at receiver position k from all sources, NTF_{ki} is the airborne noise transfer function between source i = 1, 2, 3…, L and receiver k = 1, 2, 3…, M and Q_i is the acoustic load (volume acceleration) of airborne source i. The acoustic loads can be calculated via Eq. (2) [8]:

$$Q_i^2(\omega) = [H_{j,i}^2(\omega)]^{-1} \cdot u_j^2(\omega)$$

$$(2)$$

where H_{ji} is the transfer function matrix between all sources and indication microphones j = 1, 2, 3…, N and u_j is the sound pressures at indicator microphone j. $H_{j,i}$ represents a three-dimensional matrix, defined in Eq. (3):

$$[H_{j,i}(\omega)] = \begin{bmatrix} H_{1,1}(\omega) & H_{1,2}(\omega) & ... & H_{1,L}(\omega) \\ H_{2,1}(\omega) & H_{2,2}(\omega) & ... & H_{2,L}(\omega) \\ H_{3,1}(\omega) & H_{3,2}(\omega) & \cdots & H_{3,L}(\omega) \\ \vdots & \vdots & \vdots & \vdots \\ H_{N,1}(\omega) & H_{N,2}(\omega) & ... & H_{N,L}(\omega) \end{bmatrix}$$

$$(3)$$

where each term of $H_{j,i}$ is a vector representing the transfer functions between volume sound source Q_i and indicator microphone u_j.

As an example of transfer function estimation, the first column $H_{j,1}(\omega) = [H_{1,1}(\omega) \quad H_{2,1}(\omega) \quad ... \quad H_{N,1}(\omega)]^T$ can be calculated via Eq. (4):

$$H_{j,1}(\omega) = \frac{S_{Q_1,p_j}(\omega)}{S_{Q_1,Q_1}(\omega)}, \qquad j = 1,2,3,...,N,$$

$$(4)$$

where S_{Q_1,p_j} is the cross-power spectral density and S_{Q_1,Q_1} is the auto-power spectral density. Analogously, the transfer function matrix describing the paths between all sources Q_i and all target microphones y_k is represented via Eq. (5):

$$[NTF_{k,i}(\omega)] = \begin{bmatrix} NTF_{1,1}(\omega) & NTF_{1,2}(\omega) & ... & NTF_{1,L}(\omega) \\ NTF_{2,1}(\omega) & NTF_{2,2}(\omega) & ... & NTF_{2,L}(\omega) \\ NTF_{3,1}(\omega) & NTF_{3,2}(\omega) & \cdots & NTF_{3,L}(\omega) \\ \vdots & \vdots & \vdots & \vdots \\ NTF_{M,1}(\omega) & NTF_{S,2}(\omega) & ... & NTF_{M,L}(\omega) \end{bmatrix}$$

$$(5)$$

4   HELMHOLTZ INVERSE BEAMFORMING

The following section describes the authors' algorithm for partial sound source estimation named Helmholtz Inverse Beamforming. Instead of the indicator microphones used for ASQ, as explained in section 3, the estimation of the acoustic loads with HIBF is based on a microphone array.

4.1 Helmholtz equation

Let $\bar{p} : \mathbb{R}^3 \to \bar{\mathbb{C}} = \mathbb{C} \cup \{\infty\}$ be the complex amplitude of a time-harmonic sound pressure field of angular frequency $\omega > 0$ and speed of propagation $c > 0$. By definition, $\bar{p}$ satisfies the Helmholtz equation (Eq. (6)):

$$\frac{\partial^2 \bar{p}}{\partial x^2} + \frac{\partial^2 \bar{p}}{\partial y^2} + \frac{\partial^2 \bar{p}}{\partial z^2} + k^2 \bar{p} = 0, \quad k = \frac{\omega}{c} \tag{6}$$

where $t \to exp(i\omega t)$ is used as sign convention for a time-harmonic function. Equation (7):

$$\bar{p}(x, y, z) = \frac{exp(-ik\sqrt{x^2 + y^2 + z^2})}{\sqrt{x^2 + y^2 + z^2}} \tag{7}$$

for example, represents an outgoing spherical wave originated in (0, 0, 0).

Let $p : [0, \infty] \times [0, \pi] \times [0, 2\pi] \to \bar{\mathbb{C}}$ be $\bar{p}'s$ representation in spherical coordinates (r, θ, ϕ). Consequently, p satisfies Eq. (8):

$$\frac{1}{r^2} \frac{\partial}{\partial r}\left(r^2 \frac{\partial p}{\partial r}\right) + \frac{1}{r^2 \sin \theta} \frac{\partial}{\partial \theta}\left(\sin \theta \frac{\partial p}{\partial \theta}\right) + \frac{1}{r^2 \sin^2 \theta} \frac{\partial^2 p}{\partial \phi^2} + k^2 p = 0. \tag{8}$$

Analytic solutions to this equation can be found by assuming that p is separable, i.e., there exist functions $R : [0, \infty] \to \bar{\mathbb{C}}, \Theta : [0, \pi] \to \bar{\mathbb{C}}, \Phi : [0, 2\pi] \to \bar{\mathbb{C}}$ such that Eq. (9) holds true:

$$p(r, \theta, \phi) = R(r) \cdot \Theta(\theta) \cdot \Phi(\phi). \tag{9}$$

In this case, Eq. (8) is solved uniquely by using Eq. (10):

$$R(r) = A \cdot h_l^{(1)}(kr) + B \cdot h_l^{(2)}(kr) \tag{10}$$

for some constants $A, B \in \mathbb{C}, l \in \mathbb{N}_0 = \{0, 1, \dots\}$, where $h_l^{(1)}, h_l^{(2)}$ denote the spherical Hankel functions of the first and second kind of degree l, respectively. Moreover, there is Eq. (11):

$$\Theta(\theta) \cdot \Phi(\phi) = Y_l^m(\theta, \phi) \tag{11}$$

where $m \in \{-l, -l + 1 \dots, l\}$ and Y_l^m is the spherical harmonic of degree l and order m. It is supposed p is generated in a compact ball around the origin and apply Sommerfeld's radiation condition [14] by assuming that (in the area of interest) p in Eq. (12) is (at least in good approximation) a superposition of the first $(L + 1)^2$ outgoing separable solutions of Eq. (8):

$$p(r,\theta,\phi) = \sum_{l=0}^{L} \sum_{m=-l}^{l} B_{lm} \cdot h_l^{(2)}(kr) \cdot Y_l^m(\theta,\phi), \quad B_{lm} \in \mathbb{C}. \tag{12}$$

4.2 Acoustic model

It is assumed for a moment that the total pressure field p_{tot} under consideration is a composition of N acoustic monopoles at prescribed positions $x_1, \dots, x_N \in \mathbb{R}^3$. Then, by using monopole transfer functions $t_1, \dots, t_N$, p_{tot} can be expressed in terms of the acoustic volume flow in Eq. (13):

$$p_{tot}(x) = \sum_{i=1}^{N} Q^i \cdot t_i(x). \tag{13}$$

For convenience, p is identified with $\bar{p}$ here, and is continued to do so. By rewriting this into Eq. (14):

$$p_{tot}(x) = \sum_{i=1}^{N} Q_{00}^i \cdot h_0^{(2)}(kr_x) \cdot Y_0^0(\theta_x, \phi_x) \cdot \frac{t_i(x)}{h_0^{(2)}(kr_x) \cdot Y_0^0(\theta_x, \phi_x)} \tag{14}$$

and by using the identity $Q_{00}^i = Q^i$, the monopole assumption in the spirit of subsection 4.1 can be generalized in Eq. (15):

$$p_{tot}(x) = \sum_{i=1}^{N} \sum_{l=0}^{L} \sum_{m=-l}^{l} Q_{lm}^i \cdot h_l^{(2)}(kr_x) \cdot Y_l^m(\theta_x, \phi_x) \cdot \frac{t_i(x)}{h_0^{(2)}(kr_x) \cdot Y_0^0(\theta_x, \phi_x)} \tag{15}$$

In other words, the chosen acoustic mode consists of N sources at positions $x_1, \dots, x_N \in \mathbb{R}^3$ with a total of $N \cdot (L+1)^2$ complex parameters Q_{lm}^i to model p_{tot}.

4.3 Inverse beamforming

Based on a measurement of p_{tot} and $t_1, \dots, t_N$ at the positions $x_1^m, \dots, x_M^m \in \mathbb{R}^3$ in the source-free region, it is now intended to determine/reconstruct the $N \cdot (L+1)^2$ complex numbers $Q_{lm}^i \in \mathbb{C}$ numerically. An SEM-inspired approach [15] is chosen by utilizing the so-called cross-spectral matrix C^{meas}, the matrix of auto- and cross-spectra resulting from an averaged short-time FFT of the measurement of p_{tot}. More precisely, the function in Eq. (16) is tried to be minimized:

$$F(Q_{00}^1, \dots, Q_{LL}^N) = \| C^{meas} - hh^+ \|_2^2 \tag{16}$$

where the superscript + denotes the Hermitian adjoint and h is the column vector, described in Eq. (17):

$$h(Q_{00}^1, \dots, Q_{LL}^N) = \left(p_{tot}(x_1^m), \dots, p_{tot}(x_M^m) \right)^T \tag{17}$$

with a computation by using the measured values of $t_1, \dots, t_N$ in Eq. (15). In contrast to the SEM method, a Broyden-Fletcher-Goldfarb-Shanno (BFGS) [16] minimizer with the hookstep trust region method as global strategy to minimize Eq. (16) is used.

5   EXPERIMENTS

For convenience the following description of the measurements is solely based on ASQ. Nevertheless, the same measurements must be performed for HIBF. To perform ASQ according to Fig. 2 and Eq. (1) two kinds of measurements are necessary. Firstly, the measurements intended for the calculation of the acoustic transfer function matrices $H_{j,i}$ and $NTF_{k,j}$ and secondly operational measurements for the estimation of the acoustic loads Q_i via the indicator microphones u_j. By using the acoustic loads Q_i, the SPL at the target microphones y_k can be calculated via the transfer function matrix $NTF_{k,j}$. The measurements according to the transfer function calculation are performed via a so-called Volume Velocity Source (VVS) [17] where the positions of the VVS represent substitute sound sources of different car ~~~~~~~ igure 3 shows all VVS positions and the corresponding indicator microphones u ~~~~~ y.
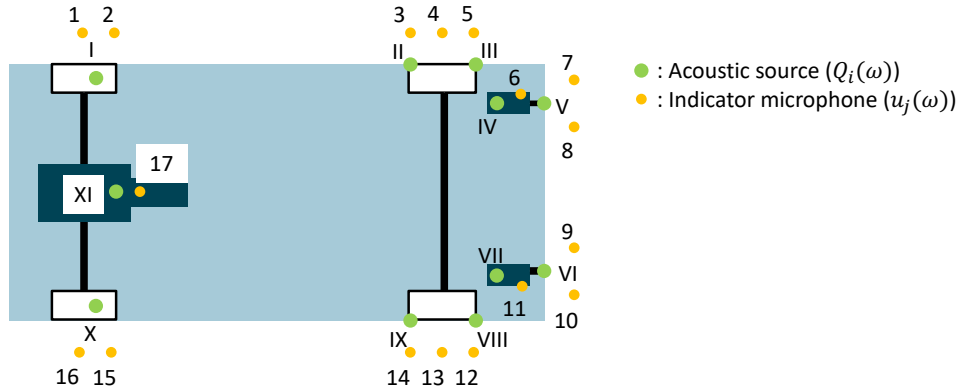

Fig. 3 Overview of all VVS positions and corresponding microphone positions for ASQ. Roman numerals stand for the number of substitute sound sources to describe the vehicles' acoustic behavior. Arabic numerals stand for the number of indicator microphones u_j to estimate the acoustic loads Q_i of the substitute sound sources. By using the pseudo-inverse of the transfer function matrix $H_{j,i}$ between all sources and all indicator microphones the acoustic loads at the VVS positions can be estimated.

The transfer function measurement consists of a logarithmic sine sweep of length $l = 60s$. Figure 4 shows the measurement arrangement and the microphone array used for HIBF.

*Fig. 4 Measurement arrangement on the indoor pass-by noise test track. **a:** Car placed on the dynometer including the microphone array for HIBF (surrounding the car) and the microphone lines for simulated pass-by (at the left and right wall). **b**: VVS (red arrow) to measure the transfer functions. **c**: Indicator microphones for ASQ.*

In a second step operational measurements in different driving conditions according to the ECE R51.03 are performed. These measurements are the basis for the comparison of the classic ASQ approach with the authors' HIBF algorithm. The comparison of the two algorithms consists of several steps:

1. Validation with VVS measurements

   a. Evaluation of four VVS measurement positions (VI, XIII, IX, XI according to Figure 3) by projecting the estimated acoustic loads to the indicator microphone positions (8, 12, 15, 17)

   b. Superposition of all sensor signals of the four VVS measurements (to simulate simultaneous sources) and evaluation at all microphone positions of 1a

2. Validation with operational measurements of a vehicle (crs in gear 4)

   a. Evaluation of all VVS measurement positions by projecting the estimated acoustic loads to the indicator microphone positions (13, 14)

As described above this study is focused on the validation of the algorithms at the indicator microphone positions. Evaluations in form of simulated pass-by noise calculations are ongoing work. All validation steps are performed for ASQ and HIBF and the results are compared. For the validation steps 1a and 1b VVS measurements are regarded as "synthetic" operational

measurements. The advantages of these measurements are the known volume velocities of the VVS and the separated SPL resulting from these volume velocities. Thus, a direct comparison of the algorithms in form of the projection of the estimated acoustic loads to the indicator microphones with the measured SPL is possible. For validation step 2a a special vehicle called "tire tester" is used. All acoustic sources (engine, mufflers, exhaust system) are physically encapsulated and thus acoustically neglected. Therefore, this vehicle can be regarded as primarily emitting tire noise. In all validation steps three subgroups are created by superposition of all time signals of the corresponding VVS positions according to Figure 3 (tires: II, III, VIII, IX, exhaust: IV, V, VI, VII, engine: I, X, XI). Finally, the energetic sum of the three subgroups is calculated.

6   RESULTS

Figure 5 shows the comparison of the results for ASQ and HIBF for the validation steps 1a and 1b.
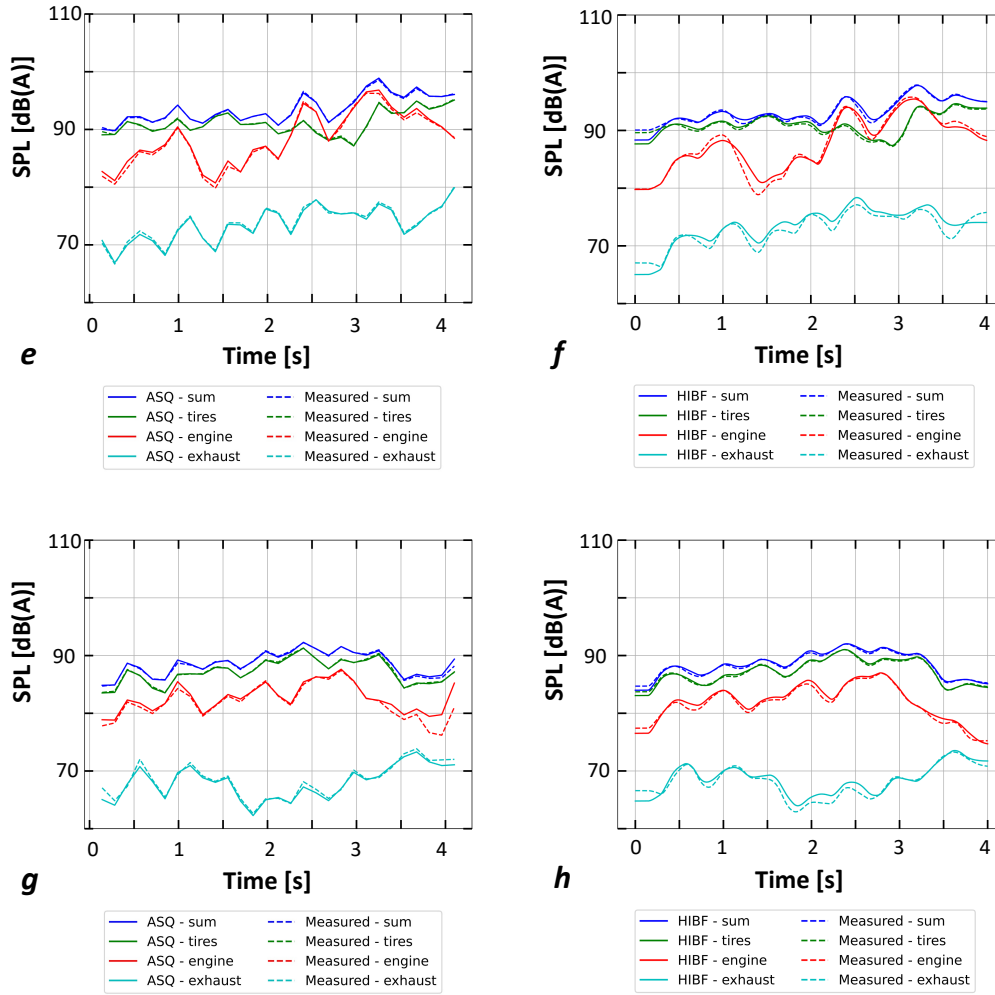

10
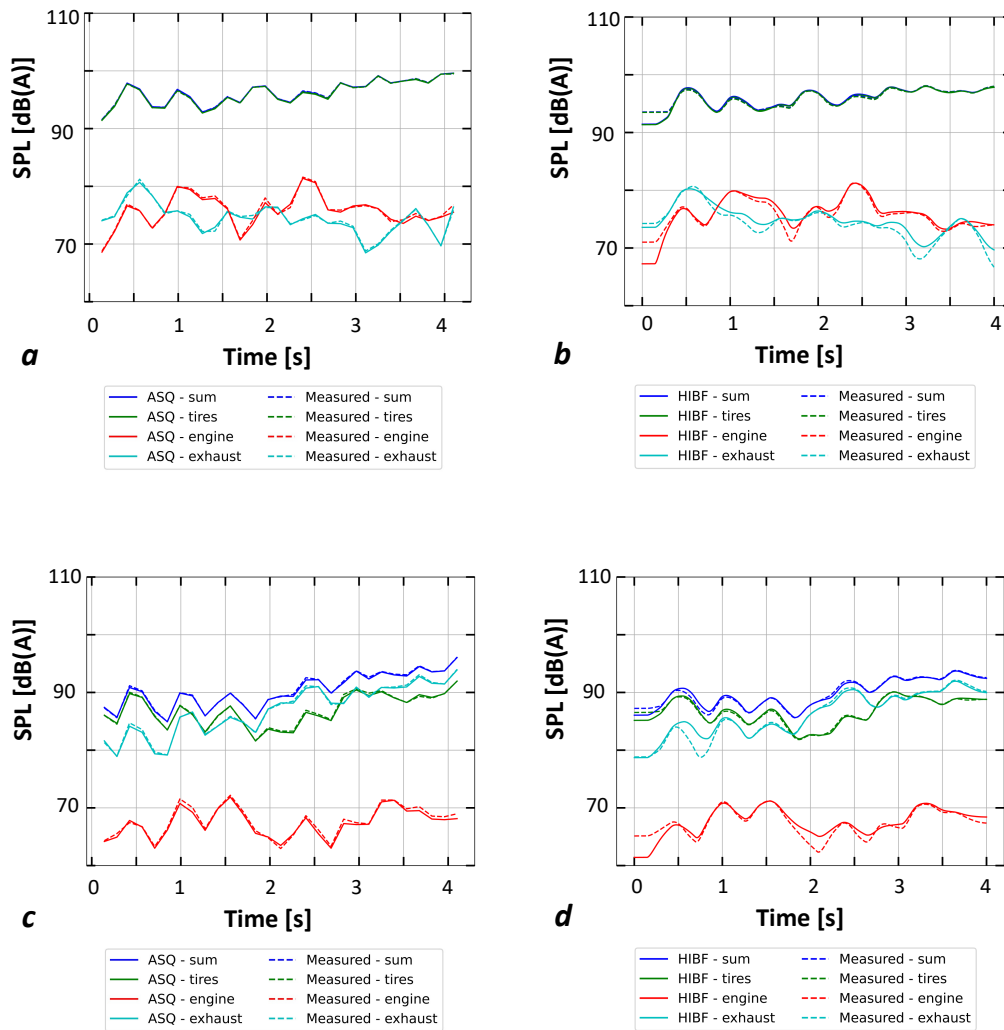
*Fig. 5 Results of VVS sinus sweep measurements for ASQ and HIBF of VVS positions VI, XIII, IX, XI (according to Fig. 3). Each subfigure shows the results of the individual measurements and the superposition. The estimated acoustic loads for the subgroups tires, engine, exhaust system and their sum are projected to an indicator microphone and compared to the measured SPL. The marginal differences in the measured signals of ASQ and HIBF (coming from identical measurements) result from a little different signal processing for RMS calculation. **a:** Projection (of the acoustic loads) to indicator microphone 12 for ASQ. **b:** Projection to indicator microphone 12 for HIBF. **c:** Projection to indicator microphone 8 for ASQ. **d:** Projection to indicator microphone 8 for HIBF. **e:** Projection to indicator microphone 17 for ASQ. **f:** Projection to indicator microphone 17 for HIBF. **g:** Projection to indicator microphone 15 for ASQ. **h:** Projection to indicator microphone 15 for HIBF.*

To get a fair comparison of ASQ and HIBF the individual indicator microphone used for the validation in each subfigure in Fig. 5 is excluded from the estimation of the acoustic loads of ASQ. The results in Fig. 5 show that for sinus sweep VVS measurements the acoustic load estimation of ASQ and HIBF is successfully working.

As a second validation step operational measurements of the tire-tester are used. In this case the real acoustic loads are unknown. Thus, the validation is only possible in an indirect way by comparing the measured SPL of the whole car with the summation of the estimated acoustic loads of the three subgroups. In a first step the results of ASQ are compared when the individual

indicator microphone used for projection is included in the acoustic load estimation and when the microphone is excluded. Figure 6 shows the results.

Figure 6 shows that for operational vehicle measurements the results of ASQ differ significantly when excluding the indicator microphone used for projection in the acoustic load estimation.
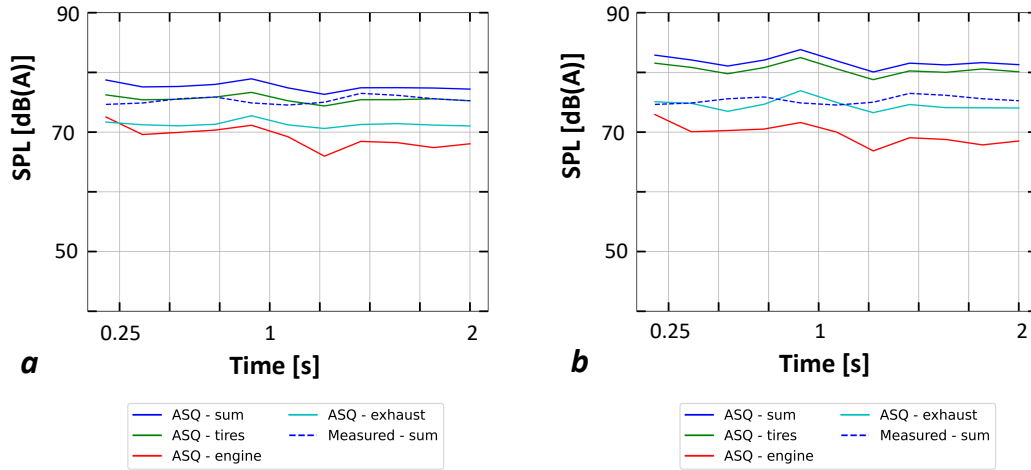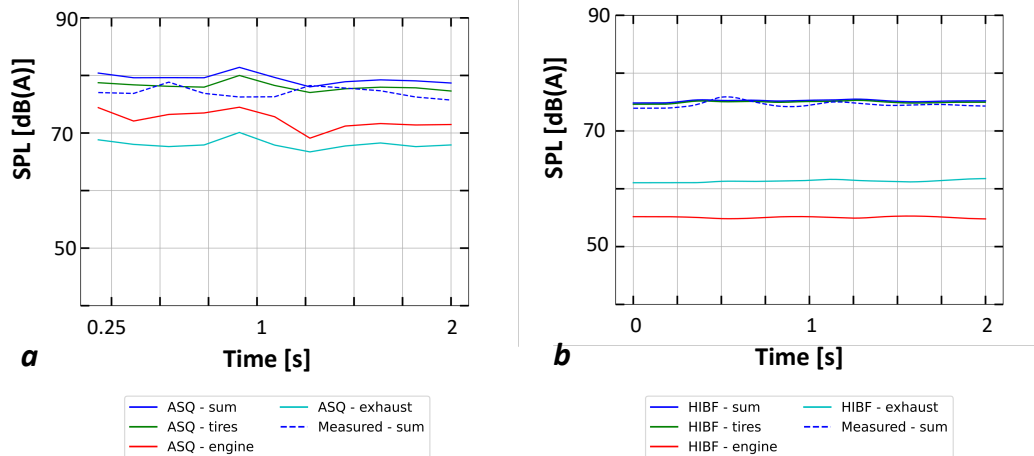

*Fig. 6 ASQ results for tire tester for the three subgroups tires, engine, exhaust, and their sum at indicator microphone 12 (according to Fig. 3). **a:** Inclusion of indicator microphone 12 for acoustic load estimation. **b:** Exclusion of indicator microphone 12 for acoustic load estimation.*

The overestimation of ASQ in form of the SPL at the indicator microphone is higher for the exclusion. For that reason, the authors decided to include the microphone for the other calculations, even though this might result in better conditions for ASQ in comparison with HIBF. Figure 7 shows the comparison of the results of ASQ and HIBF at two more microphone positions.
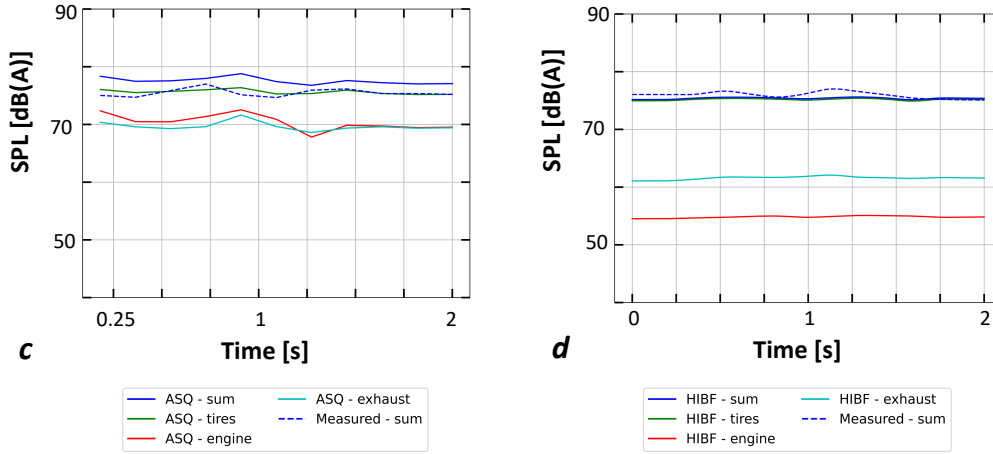
Fig. 7 Comparison of ASQ and HIBF results for tire tester for the three subgroups tires, engine, exhaust system and their sum. The marginal differences in the measured signals of ASQ and HIBF (coming from identical measurements) result from a little different signal processing for the RMS calculation. **a:** *Indicator microphone 12 for ASQ.* **b:** *Indicator microphone 12 for HIBF.* **c:** *Indicator microphone 13 for ASQ.* **d:** *Indicator microphone 13 for HIBF.*

Figure 7 shows that, analogously to Fig. 6, the sum of estimated acoustic loads projected to the indicator microphones is too loud in comparison with the measured SPL for ASQ. Additionally, the signal-to-noise-ration of the encapsulated sources engine and exhaust system in comparison with the tire noise is not that high as pass-by noise experts assumed. This leads to the assumption that engine and exhaust are overestimated in the case of ASQ. In contrast to that, the sum of the acoustic load estimation of HIBF projected to the indicator microphones matches the measured SPL almost perfectly. Additionally, the signal-to-noise-ration between tire noise versus engine and exhaust system is significantly higher compared to ASQ which leads to the conclusion that HIBF not only better matches the measured SPL but also better estimates the relation of the different acoustic loads.

7   CONCLUSIONS

In this study, the authors presented a new algorithm for partial sound source estimation for pass-by noise in hemi-anechoic test benches called HIBF. Rising legal requirements according to exterior noise of motor vehicles lead to the necessity of more precise partial sound source estimation algorithms for pass-by noise. HIBF is compared to the classical TPA approach for partial sound source estimation of pass-by noise called ASQ. For synthetic sinus sweep VVS measurements both algorithms work sufficiently precise. In contrast to that observation for operational vehicle measurements consisting of a special vehicle, where all acoustic sources besides the tires are physically encapsulated, HIBF results in a significantly lower estimation error than ASQ. Currently the authors are extending the validation of HIBF to the microphones used for simulated pass-by. Further there is ongoing work on visualization techniques for the directivity of the acoustic load estimation via HIBF. Additionally, extensive measurements with different cars are performed to further investigate the performance of HIBF for operational vehicle measurements. All algorithms according to the overlying research project are currently industrialized in a professional software application. In this context modern software concepts like software-as-a-service and cloud-based architectures are used.

8   ACKNOLEDGEMENTS

REFERENCES

[1]   Uniform provisions concerning the approval of motor vehicles having at least four wheels with regard to their sound emissions, European Standard ECE R51.03:2018. United Nations Economic Commision for Europe (UNECE), Geneva, Switzerland (2018).

[2]   Douglas Moore, "Development of ECE R51.03 noise emission regulation", SAE International, 10(3), (2017).

[3]   S. Peters, J. H. Chun and G. Lanza, "Digitalization of automotive industry - scenarios for future manufacturing", *Manufacturing Review,* **3**, 1-8, (2016).

[4]   M. Fazal-Baqaie, F. Knappe, R. Sperber, "Wie laut ist der Digitale Zwilling? - Agile Digitalisierung von Produktentstehungsprozessen am Beispiel der Außengeräusch-Homologation als Kombination von akustischen Methoden und KI", 16th Symposium für Vorausschau und Technologieplanung, (2022).

[5]   F. Knappe, C. Puhle, J. Rosskopf, "Der digitale akustische Zwilling – Ableitung von Komponenten-Grenzwerten für die Außengeräusch-Homologation in der digitalen Phase des Fahrzeugentwicklungsprozesses, DAGA, (2022).

[6]   F. Knappe, J. Rosskopf and M. Vorländer, "Pass-by Noise Prediction with Gradient Boosted Models as a Part of the Acoustical Digitalization of Automotive Product Development Processes, 13th Aachen Acoustics Colloquium, (2021).

[7]   D. Fernandez Comesana, K. Holland, J. Wind and H.-E. De Bree, "Comparison of inverse methods and particle velocity based techniques for transfer path analysis", Acoustics, (2012).

[8]   K. Janssens, F. Bianciardi, L. Britte, P. Van de Ponseele and H. Van der Auweraer, "Pass-by noise engineering: a review of different transfer path analysis techniques", *ISMA, International Conference on Noise and Vibration Engineering, 3923-3940,* (2014).

[9]   F. Bock, M. Pohl, D. Arsić and S. Becker, "A statistical analysis of the influence of a vehicles exterior appearance on exterior noise," *Aachen Acoustics Colloquium,* (2016).

[10]   D. Arsić and M. Pohl, "A framework for the sensitivity analysis of transfer paths combining contribution analysis and response modification analysis," *Automotive Acoustics Conference, 341–351*, (2019).

[11]   B. D. Van Veen and K. M. Buckley, "Beamforming: a versatile approach to spatial filtering", *IEEE ASSP Magazine*, **10**(2), (1988).

[12]   *Acoustics–Measurement of noise emitted by accelerating road vehicles – Engineering method*, International Standard ISO 362:1998, International Organization for Standardization, Geneva, Switzerland, (1998).

[13]   J.W Verheij, "Inverse and reciprocity methods for machinery noise source characterization and sound path quantification, part 1: sources", International Journal of Acoustics and Vibration **2**(1), *11-20*, (1997).

[14]   A. Sommerfeld, "Partial differential equation in physics", *Pure and Applied Mathematics,* **1,** (1949).

[15]   D. Blacodon and G. Élias, "Level estimation of extended acoustic sources using a parametric method", *Journal of Aircraft,* **41**(6), *1360-1369,* (2004).

[16]   C.T. Kelley, "Iterative methods for optimization", SIAM, (1999).

[17]   Siemens LMS, "What is the acoustic quantity called Q", Siemens Community Article, (2019), https://community.sw.siemens.com/s/article/what-is-the-acoustic-quantity-called-q